ACS PHYSICAL CHEMISTRY Au
AN OPEN ACCESS JOURNAL OF THE AMERICAN CHEMICAL SOCIETY

pubs.acs.org/physchemau
Article

Effect of Organic Coating Variation on the Electric and Magnetic Behavior of Ferrite Nanoparticles

Nikolaos Ntallis and Kalliopi N. Trohidou*

Cite This: ACS Phys. Chem Au 2023, 3, 532−539
Read Online

ACCESS | Metrics & More | Article Recommendations | Supporting Information

ABSTRACT: Organic ligand coatings can modify the surface properties of nanoparticles. With the proper choice of the type of nanoparticles and of the ligand, a targeted modification can be achieved that is suitable for specific applications. In the present work, we employ density functional theory calculations with Hubbard corrections (DFT + U) to treat localized states in order to investigate the magnetic and electrostatic properties of ferrite nanoparticles ($CoFe_2O_4$ and Fe_2O_3) covered with COOH-terminated [oleic acid (OA)] and OH-terminated [diethylene glycol (DEG)] ligands by varying the ligands coverage. OA results in a decrease of the mean magnetic moment for both particles as the coating coverage increases. The magnetic anisotropy (MAE) significantly decreases for $CoFe_2O_4$, whereas for Fe_2O_3 a significant increase of MAE is found as the OA coverage percentage increases. For DEG, the variation of both types of nanoparticles in the magnetic moment and the magnetic anisotropy is not significant since DEG shows a weaker attachment on the surface. As COOH shows a larger percentage of covalent bonding than OH, a larger amount of charge is transferred to both particles when OA is attached on their surface. In this case, the particles possess a higher charge, and thus they can produce a larger electrostatic potential in the neighborhood independently of the screening by the coating. Thus, the repulsive Coulombic forces are enhanced mainly in the OA coating case, resulting in an enhancement of their colloidal stability.

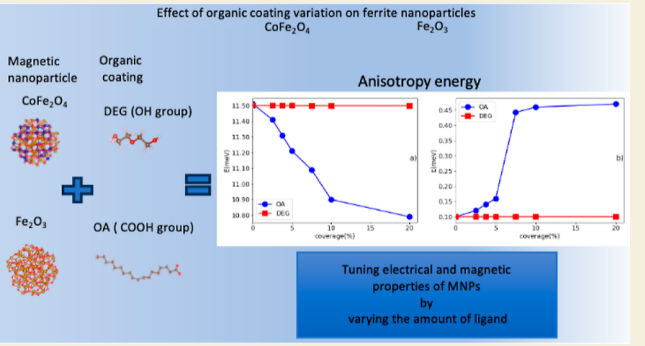

KEYWORDS: *magnetic nanoparticles, organic coating, DFT, magnetic interactions, colloidal dispersions*

1. INTRODUCTION

In the last few years, magnetic nanoparticles (MNPs) have gained great interest in the fields of biomedicine,[1,2] environment,[3] and energy[4] as solid nanostructures and ferrofluids.[5,6]

Nanotechnology enables the production of MNPs with specific morphologies and the tailoring of their surfaces in order to manipulate their characteristics for specific applications. In the nanoscale, the nanoparticles are usually prepared with colloidal synthesis that uses surfactants in order to obtain a narrow size and shape distribution but also to functionalize them for specific applications, such as biomedical ones (e.g., MRI, drug delivery, and hyperthermia).[1]

The choice of organic coating is of great importance since it affects the magnetic properties of the nanoparticles.[7] The presence of a surfactant can alter the surface ion distribution[8] and from magnetic point of view the surface spin arrangement.[9] It may also influence the local effective magnetic anisotropy,[8] the exchange coupling constants between the surface spins,[8] and the particle saturation magnetization.[8] As a result, different ligands bonded at the surface of the MNPs affect the magnetic behavior and colloidal stability.[10]

The interest in coated MNPs focuses on the understanding of the underlying mechanisms by which surfactant molecules contribute to their magnetic properties. Such an exercise is quite demanding, as there is a large number of parameters to be investigated. The effect of the coating depends on the type of coating, the type of particles (structure, size, shape), and also the amount of coating coverage on the particles' surface.[11−13] Theoretical studies[14,15] have shown that different percentages of small organic or CO molecules attached at the surface of small Co clusters can alter their magnetic properties.

In recent years, nanoscale transition-metal (TM) oxides, such as iron oxides, including hematite, magnetite, and maghemite, have attracted growing interest as they exhibit unique electrical, optical, and magnetic properties for numerous applications such as production of magnetic storage media, development of sensors as well as electronic and optical devices, bioprocessing, and ferrofluids technology.[16] Among the different types of ferrites, γ-Fe_2O_3 nanoparticles have been

Received: June 6, 2023
Revised: September 21, 2023
Accepted: September 22, 2023
Published: October 19, 2023

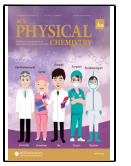

extensively used in technological applications and in hyperthermia. Co ferrite nanoparticles are considered among the most promising materials for biomedical (hyperthermia, MPI), environmental, and technological applications[17,18] because of their high magneto-crystalline anisotropy.

Oleic acid (OA) is commonly used as a coating in ferrite nanoparticles as it provides their steric stabilization and most importantly reduces the toxic effects of some of these nanoparticles in various applications.[19]

Theoretical works[20,21] have demonstrated that the bulk magnetization of Fe_3O_4 films[20] and Fe_3O_4 orthogonal-shaped nanoclusters[21] can be restored when specific covalently bonded ligands are attached to the surface by specific binding modes (i.e., monodentate, bidentate, etc.). More specifically, in these works OA[20] and acetic acid[21] coatings (both possessing a COOH group) prefer a bidentate binding mode. In ref 20, the directly bonded atoms show an enhanced magnetic moment due to the reconstruction of the original bulk O environment around the TM atoms. This mode is also responsible for an additional ferromagnetic super exchange that enhances the NP magnetization.[21] Experimental results of the effect of the OA coating concentration on the magnetic behavior of the Co ferrite nanoparticles by Limaye et al.[22] showed that as the concentration of OA increases, the coercivity also increases. On the other hand, Jovanović et al.[23] found that the OA covalently bonded to the Co ferrite nanoparticle surface decreases the surface anisotropy and the coercive field of OA-coated nanoparticles with the increase in the OA surface coverage.

Another typical coating is glycol in the form of DEG or triethylene glycol (TEG). The main difference between OA and glycols is their functional group, i.e., COOH for OA and OH for glycol. The difference of the functional group may lead to different functionalization as it results in different types of binding. The type of binding also affects the partial charge of the surface atoms and, thus, the electrostatic field produced by the particle. Moreover, the different coatings, due to the different molecular weights, can produce different screenings of the electrostatic potential. In this sense, the different ligands can change the electrostatic forces between the particles and therefore their stability in an assembly.

In this work, we investigate the effect of two different coatings, OA and DEG, on two ferrite spherical nanoparticles, γ-Fe_2O_3 and $CoFe_2O_4$. In order to shed light on the influence of the coating on the magnetic and electrostatic behavior of the nanoparticles, we perform density functional theory (DFT) calculations on these two types of nanoparticles with an increasing amount of ligand coverage for nanoparticles with a diameter ∼2 nm, from 0 to 20% surface coverage. We study the effect of the type of nanoparticles, the type of coatings, the surface coverage percentage of the saturation magnetization, and the magnetic anisotropy. We also study the effect of the coatings on the charge distribution of the nanoparticles and of their electrostatic potential.

2. MODELING AND SIMULATION METHODS

DFT calculations were performed based on spin-polarized density functional theory implemented by the Vienna ab initio simulation package (VASP) code,[24,25] in a spinel ferrite with stoichiometric chemical formulas $CoFe_2O_4$ (inverse spinel) and Fe_2O_3 (spinel). In both structures, O atoms are arranged in a closed packed cubic FCC structure and create tetrahedral sites named A sites and octahedral sites named B sites.[26] The TM ions fill some or all of these sites. For $CoFe_2O_4$, Co ions (Co^{2+}) occupy 1/8 of the B sites, whereas Fe (Fe^{3+}) atoms occupy 1/8 of the B sites and 1/4 of the A sites. For Fe_2O_3, Fe atoms occupy 1/4 of the A sites (Fe^{3+}) and 0.15 of the B sites (Fe^{3+}). In our calculations, the electronic charge density and the local potential were expressed in plane wave basis sets. The chosen exchange correlation functional was the one proposed by Perdew–Burke–Ernzerhof (PBE). The interactions between the electrons and ions were described using the projector-augmented-wave (PAW) method and the GGA + U approach to treat localized states as proposed by Dudarev et al.[27] For the effective exchange parameter U_{eff}, values of 4.5 eV for Fe and 4.0 eV for Co atoms for $CoFe_2O_4$ and a value of 4 eV for Fe in Fe_2O_3 were found. The initial structures were formed by replication of the bulk unit cell, followed by a trimming procedure in order to obtain the spherical shape for the nanoparticles. The resulting structures are spherical nanoparticles with a diameter D ∼ 2 nm. Moreover, an empty space of 1.5 nm is used in all directions in order to avoid interaction with periodic images. For these nanoparticles, different numbers of bonded monomers per nanoparticle's surface area were considered for the different percentages of surface coverage. Coverage is defined as the ratio of the monomers attached to the surface with respect to the number of surface atoms, which is defined as the atoms of the outer layer of the nanoparticle. The spins of TM ions between sites A and between sites B are ordered ferromagnetically (FM) and antiferromagnetically (AF) between A–B sites in the initial spin configuration. By applying the Bader charge analysis scheme,[28] we can estimate the charge per atom and also the total charge of the particle after the addition of the coating. Moreover, from the calculated charge density, we can extract the electric field produced by the particle in space. The charge of each atom is taken as

$$q = q_c - q_v \quad (1)$$

where q_c is the calculated Bader charge and q_v the valence charge of each atom. In order to have an accurate estimation of the charges, we employ DFT calculations with progressively increasing the density of the real space fast Fourier transform grid used to represent the augmented pseudo charge densities in order to obtain in this way a difference in charges smaller than $10^{-3}e$.

3. RESULTS AND DISCUSSION

3.1. Binding Energies

Figure 1 shows relaxed structures of $CoFe_2O_4$ coated with OA (Figure 1a), coated with DEG (Figure 1b) and Fe_2O_3 coated with OA (Figure 1c) and coated with DEG (Figure 1d). In Figure 1, the structures include only one molecule attached to the surface. Relaxed structures of the highest coverage percentage are shown in the Supporting Information.

In order to identify the first binding mode, we performed the relaxation with ligands placed on the top of different ions on the surface of the $CoFe_2O_4$ nanoparticle. For DEG monomers, only a monodentate mode was considered, whereas for OA, both the monodentate and the bidentate mode were considered. In all cases, the monodentate mode was found to be more stable, which contradicts the corresponding behavior of refs 20 and 21, where for ligands with COOH groups, the bidentate mode is energetically favored for orthogonal-shaped structures.

A major difference between orthogonal and spherical nanoparticles is the surface structure, which is related to the number of surface atoms that have reduced number of neighbors, with the coordination number of surface spins of spherical nanoparticles being smaller than that of the orthogonal shape.[29] This difference indicates that the attachment of the coating strongly depends not only on the size of the NPs, as a very large size will tend to recover the bulk behavior, but also on their morphology. As monodentate mode

https://doi.org/10.1021/acsphyschemau.3c00026
ACS Phys. Chem Au 2023, 3, 532–539

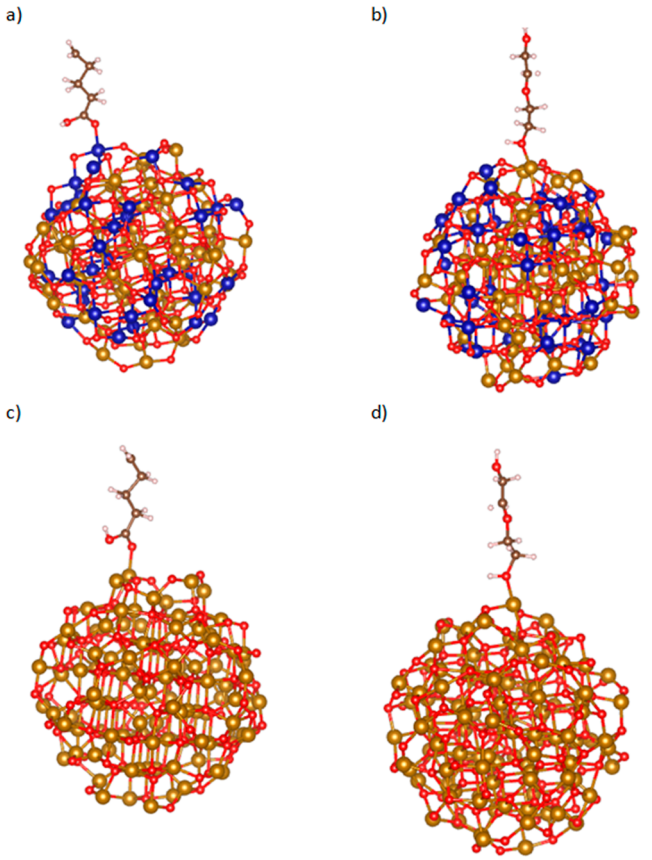

Figure 1. Relaxed structures of $CoFe_2O_4$ particles with (a) 1 OA monomer, (b) 1 DEG monomer and Fe_2O_3 particles with (c) 1 OA monomer, (d) 1 DEG monomer. For clarity, OA is not shown as a whole. Color code of atoms is yellow for Fe, blue for Co, red for O, brown for C, and white for H.

was the one used in our calculations, it is the only one discussed here. However, for comparison the bidentate mode is also shown in Supporting Information.

The lowest energy state is found when the OA is directly bonded by an O from its COOH group with a Co atom with a Co−O distance of 1.68 Å. In the case of the DEG coating, the lowest ground state is found when the O from its OH group is at an Fe−O distance of 2.10 Å on top of a Fe ion. For Fe_2O_3, the lowest energy ground state is found when OA is placed on top of an initially placed octahedral (B) site with a Fe−O distance of 1.70 Å, whereas the DEG on top of a tetrahedral (A) site with a Fe−O distance of 2.20 Å. This bond distance difference between ligand(s) and nanoparticle structure indicates that OA has a higher covalent bond character from DEG in both nanoparticles. From Bader charge analysis, we find that the charge of TM atoms is reduced when OA is attached in both types of nanoparticles, whereas for DEG it is almost unaffected. Table 1 shows the Bader charge q of the TM atoms before and after the addition of coating for both $CoFe_2O_4$ and Fe_2O_3 nanoparticles. For the $CoFe_2O_4$ nanoparticle and OA coating, the Co atom type shows a larger reduction of q, indicating a larger charge transfer to the bond with respect to the Fe atom type and therefore a stronger binding. In Fe_2O_3 nanoparticles, the Fe atoms that bonded atoms with OA show a reduced charge and are smaller than the Co and Fe atoms of $CoFe_2O_4$ nanoparticle. Therefore, a smaller amount of charge is transferred to the bond in this

Table 1. Bader Charge of TM Atoms before and after the Addition of Coating for Both $CoFe_2O_4$ and Fe_2O_3 Nanoparticles

nanoparticle	coating	TM atom type	q (e)
$CoFe_2O_4$		Fe	1.51
$CoFe_2O_4$	OA	Fe	1.42
$CoFe_2O_4$	DEG	Fe	1.50
$CoFe_2O_4$		Co	1.12
$CoFe_2O_4$	OA	Co	0.95
$CoFe_2O_4$	DEG	Co	1.01
Fe_2O_3		Fe	1.54
Fe_2O_3	OA	Fe	1.49
Fe_2O_3	DEG	Fe	1.53

case. This charge reduction verifies that the bond has a larger covalent character.

The latter holds from an energetic point of view also. This can be clearly seen in Table 1, with the binding energy E_b, defined as $E_b = E_t - E_p - E_L$, with E_t the energy of the particle-ligand system, E_p the isolated particle energy, and E_L the isolated ligand energy (Table 2).

Table 2. Binding Energy E_b for One OA or DEG Monomer Attached to the $CoFe_2O_4$ and Fe_2O_3 Nanoparticles

nanoparticle	coating	E_b (eV/atom)
$CoFe_2O_4$	OA	−0.811
Fe_2O_3	OA	−0.715
$CoFe_2O_4$	DEG	−0.223
Fe_2O_3	DEG	−0.431

Next, we plot the binding energy for the two types of nanoparticles as a function of the surfactant coverage for $CoFe_2O_4$ (Figure 2a) and Fe_2O_3 (Figure 2b) particles.

$CoFe_2O_4$ shows the highest binding energy for both coatings with respect to Fe_2O_3. Interestingly, in the Fe_2O_3 system for the OA coating E_b shows a small increase for a very small coating percentage (∼7.5%) and gradually, as the coverage increases, reaches an almost constant energy value, indicating that binding becomes less favorable as the OA coating increases. As both nanoparticles share the same crystal structure, the presence of Co is the one that makes the binding more favorable for $CoFe_2O_4$ than Fe_2O_3. Both structures have Fe ions in B sites. Due to the inverse spinel structure in $CoFe_2O_4$, Co atoms are initially placed in B sites. Co atoms on average have a larger number of O atoms on the surface rather than the Fe atoms initially placed in A sites. This is also verified by the mean Co−O distance which is calculated to be ∼1.95 Å in contrast to that of Fe−O, which is ∼1.85 Å. Thus, Co is in a slightly higher ionic state and can create stronger bonds.

3.2. Magnetic and Electrostatic Properties

Table 3 shows the mean value of the magnitude of the magnetic moment per TM atom type for the two nanoparticle systems in the case of only one molecule attached on the surface of the nanoparticle. In the parentheses are given the corresponding values of the uncoated particles from our calculations.

Even though these calculations were performed for only one molecule attached on the surface of the particle, a larger reduction of the magnetic moment is found per atom type in the case of the OA coating compared to that of the DEG

https://doi.org/10.1021/acsphyschemau.3c00026
ACS Phys. Chem Au 2023, 3, 532−539

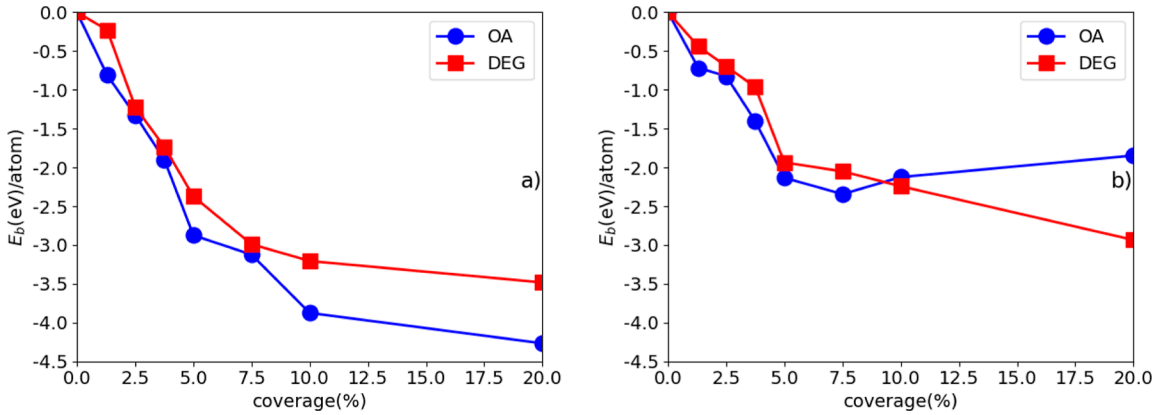

Figure 2. Binding energy E_b with respect to the coverage percentage for the two coatings (a) $CoFe_2O_4$ and (b) Fe_2O_3 nanoparticle systems.

Table 3. Mean Value of the Magnitude of the Magnetic Moment per TM Atom Type for the Two Nanoparticle Systems

nanoparticle	coating	atom type	M (μ_B)
$CoFe_2O_4$	OA	Fe	4.15 (4.41)
$CoFe_2O_4$	OA	Co	2.71 (2.75)
Fe_2O_3	OA	Fe	4.12 (4.32)
$CoFe_2O_4$	DEG	Fe	4.42 (4.41)
$CoFe_2O_4$	DEG	Co	2.73 (2.75)
Fe_2O_3	DEG	Fe	4.32 (4.32)

coating. Such a reduction is observed in not only the directly ligand-bonded TM atom but also in the nearby TM ones. For $CoFe_2O_4$, the directly bonded Co atom shows a reduction of 0.04 μ_B, whereas the nearby Co ones show a reduction of 0.02 μ_B. Nearby Fe atoms show a larger reduction reaching 0.3 μ_B.

Figure 3 shows the mean magnetic moment M for the $CoFe_2O_4$ nanoparticle (Figure 3a) and Fe_2O_3 (Figure 3b) with respect to the coverage percentage. For M, only the TM atoms are included. There is a significant decrease in the coverage in the case of the OA coating in both types of nanoparticles. For the DEG coating, the difference is almost negligible.

As the coverage percentage increases, M gradually reduces in the case of OA coating. For small coverage concentrations (<5%), M shows a slower reduction in the $CoFe_2O_4$ from that in the Fe_2O_3 nanoparticle. Overall, for $CoFe_2O_4$, the reduction for 20% coverage is 4.5%, whereas the reduction for Fe_2O_3 is 9.5%. Moreover, even though the coverage percentage is small, the Fe_2O_3 nanoparticle shows a larger gradient of reduction. The latter indicates that the Fe_2O_3 nanoparticle will probably show a larger relative reduction of the magnetic moment with respect to the $CoFe_2O_4$ one. In the case of DEG, M remains almost constant, with variation less than 0.05%, indicating again a small percentage of covalent bonding of DEG.

The magnetic anisotropy energy (MAE) in the ground state of the system is calculated for several spin orientations, taking into account the spin−orbit coupling (SOC) by rotating all spins coherently along different directions. The directions chosen ranged from 001 to 100 in steps of $\pi/10$. The energy difference between the lowest energy (easy axis) and highest energy (hard axis) provides the MAE energy of the system. A conversion from cubic to uniaxial anisotropy has already been reported for small nanoparticles.[29] In our calculations, the anisotropy was always found to be uniaxial and more specifically along the Cartesian z axis. Interestingly, regardless of the amount of coverage, this orientation did not change at all. Thus, the coverage can affect only the strength of the anisotropy and not the easy axis direction. Figure 4 shows the MAE for $CoFe_2O_4$ (Figure 4a) and Fe_2O_3 (Figure 4b) with respect to the coverage percentage for the two types of coating.

For OA, $CoFe_2O_4$ has a clear reduction of MAE with an increasing coverage percentage. By inspecting SOC elements, the reduction of the MAE is mainly due to Co atoms, as the local MAE of surface atoms reduces from 0.10 to 0.06 meV for 20% coverage. Such a decrease is found as the mean TM-O distance increases by ∼12% and thus decreasing the crystal

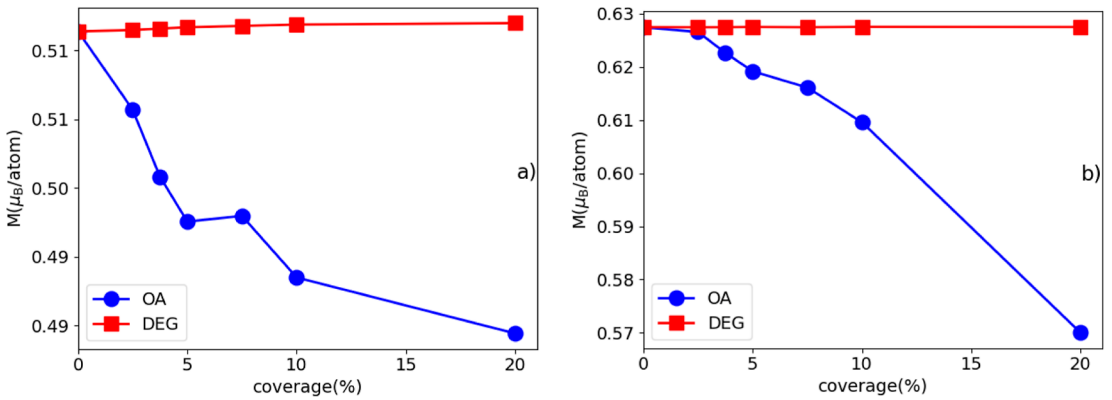

Figure 3. Mean magnetic moment of a (a) $CoFe_2O_4$ and (b) Fe_2O_3 nanoparticle as a function of the percentage of the surface coverage, for the two types of coating.

https://doi.org/10.1021/acsphyschemau.3c00026
ACS Phys. Chem Au 2023, 3, 532−539

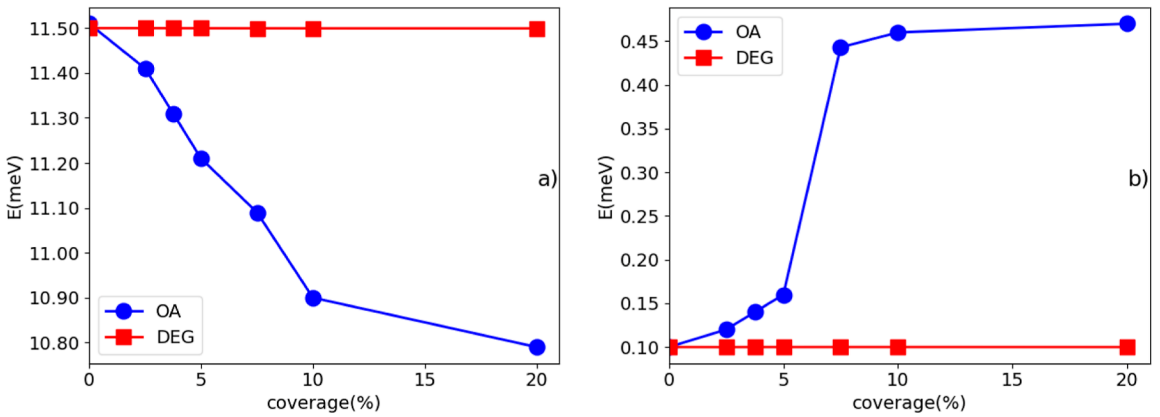

Figure 4. MAE for (a) $CoFe_2O4$ nanoparticle and (b) Fe_2O_3 nanoparticle with respect to the coverage percentage for the two types of coating.

field interaction of TM atoms with the surrounding O. As can be seen in Figure 4b, there is a noticeable enhancement of the MAE with the increase of coverage in Fe_2O_3 which is close to 75% for 5% of OA coverage and becomes ∼4.5 larger than the anisotropy of pure Fe_2O_3 at 20% of OA coverage. The local MAE of surface Fe atoms in Fe_2O_3 is increased from 0.012 meV up to 0.045 meV. As in the case of $CoFe_2O_4$ on the surface atoms, the TM-O distance increases when OA coverages increases. In the case of Fe_2O_3, this increase is smaller and calculated to be ∼8%, so one would expect the same behavior of MAE. It has to be noted here that the absolute value of MAE is still small compared to the $CoFe_2O_4$ one.

Our study on the charge of the atoms has demonstrated a reduction of the TM atom charge and an increase of the O atoms charge. For Fe_2O_3, the O charge enhancement is higher due to the stronger delocalization of Fe. Thus, the Coulombic attraction counterbalances the orbital overlap reduction and increases the crystal field interaction between TM and O atoms. The latter has, as an effect, considerable enhancement of the MAE for Fe_2O_3.

By mapping different noncollinear magnetic states on a Heisenberg Hamiltonian, we can calculate the exchange interaction constants J_{ij} between atoms i and j. The Hamiltonian used here is

$$H = -\sum_{i \neq j} J_{ij} \vec{S}_i \vec{S}_j \tag{2}$$

where $\vec{S}_i$ and $\vec{S}_j$ are the magnetic moment vectors of the neighbor atoms i, j. The different magnetic states are calculated under the constraint of the constant magnetic moment norm in order to include as energy difference only the one arising from the different angle between two neighboring atoms. In ferrites, three main different exchange interaction constants can be identified. The one between A−B atoms, the one between B−B atoms, and the one between A−A atoms. On the surface of the particles, both A and B sites possess reduced oxygen coordination with respect to the bulk. These atoms can be named as pseudo A (A′) and pseudo B (B′).

Table 4 and 5 show the calculated J_{ij} of the two particles before and after the addition of the surfactants, under the highest coverage percentage case, for Table 4 $CoFe_2O_4$ nanoparticle and the Table 5 Fe_2O_3 nanoparticle. The J_{ij} values reported here are the mean values from all interaction types on the surface of the particle.

Table 4. J_{ij} Values for $CoFe_2O_4$ Nanoparticles

uncoated		
site i	site j	J_{ij} (meV)
FeA′	FeA′	−0.86
FeB′	FeB′	1.61
CoB′	CoB′	1.45
FeA′	CoB′	−3.12
FeB′	CoB′	1.71
FeA′	FeB′	−2.93

DEG			OA		
site i	site j	J_{ij} (meV)	site i	site j	J_{ij} (meV)
FeA′	FeA′	−0.84	FeA′	FeA′	−0.85
FeB′	FeB′	1.59	FeB′	FeB′	1.34
CoB′	CoB′	1.43	CoB′	CoB′	1.18
FeA′	CoB′	−3.08	FeA′	CoB′	−3.25
FeB′	CoB′	1.69	FeB′	CoB′	1.51
FeA′	FeB′	−2.91	FeA′	FeB′	−2.91

Table 5. J_{ij} Values for Fe_2O_3 Nanoparticles

uncoated		
site i	site j	J_{ij} (meV)
FeA	FeA	−0.94
FeB	FeB	1.41
FeA	FeB	−3.15

DEG			OA		
site i	site j	J_{ij} (meV)	site i	site j	J_{ij} (meV)
FeA	FeA	−0.91	FeA	FeA	−0.91
FeB	FeB	1.38	FeB	FeB	1.11
FeA	FeB	−3.13	FeA	FeB	−3.21

In all cases, the A′−B′ antiferromagnetic interaction is the dominant one, creating the ferrimagnetic magnetic state of the ferrite nanoparticles. In contrast to the magnetic moment and magnetic anisotropy, both surfactants affect the exchange interactions, indicating a more sensitive property with respect to the interaction to the surfactant. For the DEG case, we observe a small reduction in all parameters independently. According to the binding energy, we identified a small percentage of covalent bonds for DEG and thus no direct effect on electron overlap. Thus, the reductions on J_{ij} are attributed only to electron directionality due to Coulombic form. On the other hand, interestingly OA acid shows different behavior. The AF interactions between A′−B′ sites in both systems are increased, indicating an enhanced AF order with

https://doi.org/10.1021/acsphyschemau.3c00026
ACS Phys. Chem Au 2023, 3, 532−539

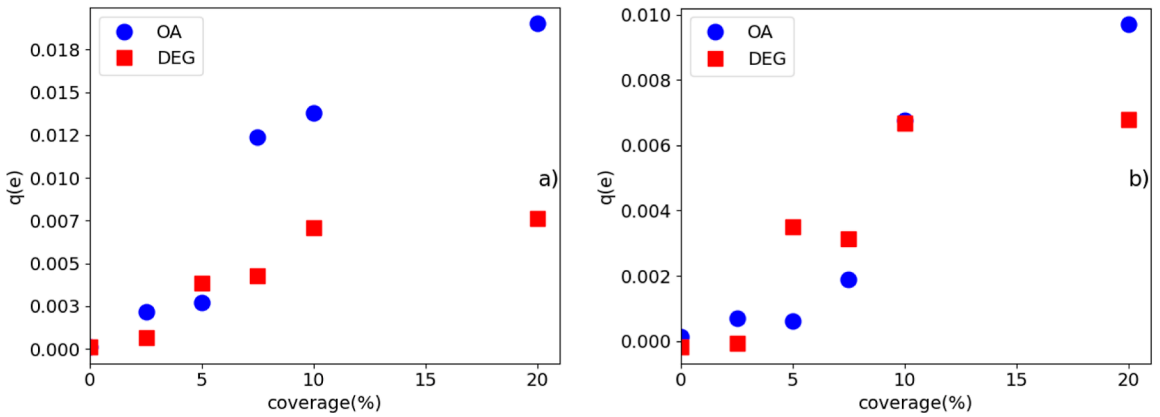

Figure 5. Total charge of OA-coated particles and (a) $CoFe_2O_4$- and (b) Fe_2O_3-coated particles with respect to the coverage percentage.

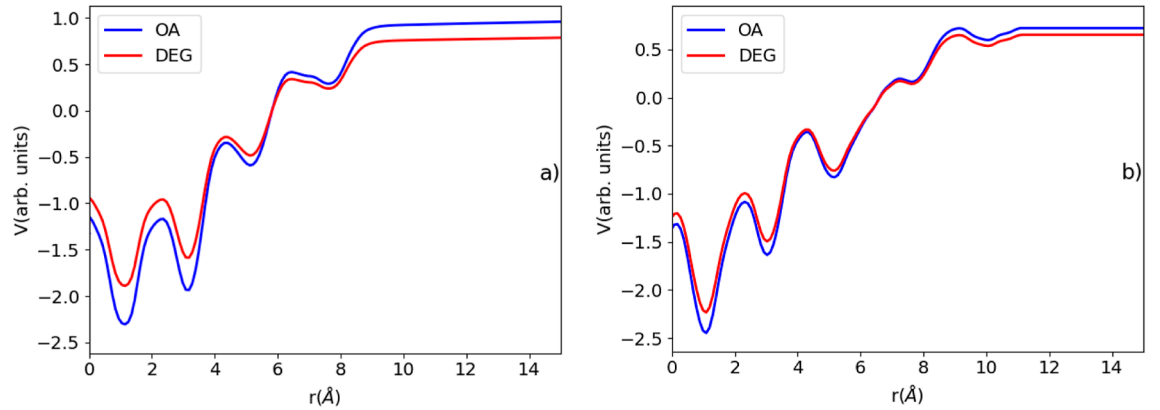

Figure 6. Average electrostatic potential for (a) $CoFe_2O_4$ particle and (b) Fe_2O_3 particle.

respect to the uncoated case. On the other hand, the A′−A′ and B′−B′ interactions decrease. Such a case indicates that the A′−B′ interactions dominate in the coated systems, thus possibly producing a more ordered magnetic state on the surface, reducing frustration even at this low coverage percentage. The B′−B′ constants can lead to a reduction of the Curie temperature of the coated particles.

As the coatings can change, the charge distribution of nanoparticles can also affect the electrostatic interactions between them. By calculating the q values per atom (see Methods) from 1 we find the total charge of the particles. The net charge of the particles is the sum of the positively charged TM atoms and the negatively charged O atoms. Figure 5 shows the total charges of $CoFe_2O_4$-coated particles (Figure 5a) and Fe_2O_3-coated particles (Figure 5b) in units of electrons with respect to the coverage percentage.

Both particles become positively charged as the coverage percentage increases. The OA shows the largest increase of charge for both particle types, indicating that more electrons are shared from the OA coating to the particle than from the DEG coating. This effect is more pronounced in the $CoFe_2O_4$ particle where a total charge of $0.02e$ is found for 20% OA coverage. Notably, the charge variation of the Fe_2O_3 nanoparticle coated with OA is not monotonic as in the $CoFe_2O_4$ particle. In the region from 2.5 to 8% coverage percentage, the particle charge shows a reduction but still maintains a positive value. This charge reduction indicates a strongly negatively charged oxygen shell on the surface, with respect to the uncoated case. For the Fe_2O_3 case and the 2.5 to 8% region of coverage, we observe that OA can bind in a carboxylate form rather than a carboxylic one. Thus, the hydrogen from the COOH group is attached to the nearby O of the TM atom (only Fe in this case). Such a case results in a higher (negative) ionic state of the oxygen shell and thus an even smaller increase of the nanoparticle's net charge. By further increasing the coverage percentage, this phenomenon is not evident anymore, and thus the slope of the charge variation of the nanoparticle gains a higher value. This behavior results in a higher charge of the DEG-coated particles in the 2.5 to 8% coverage percentage region, even though DEG shows a weaker binding to the surface with respect to OA.

The charge distribution for these structures has been used for the calculation of their electrostatic potential by solving the Poisson equation. Figure 6 shows the average electrostatic potentials of the $CoFe_2O_4$ (Figure 6a) and Fe_2O_3 (Figure 6b) samples as a function of the distance from the center of the particle. Our calculations show that all structures have the same sign of potential outside the particle, therefore we expect that their net charge also has the same sign. The value of the potential outside the particle can be considered as the zeta potential,[30] which is a measure of the strength and the range of the electrostatic interactions outside the nanoparticle. For both structures, the OA coating shows the larger value of this potential; thus, it is the one with the strongest electrostatic interaction strength, and it will more easily prevent the particles' agglomeration. In general, OA will disperse the nanoparticles in a solvent due to the aliphatic chain interactions. But such a collapse of the system can occur due to the attractive van der Waals interactions increasing the size of the particles and temperature.[31] For the $CoFe_2O_4$

https://doi.org/10.1021/acsphyschemau.3c00026
ACS Phys. Chem Au 2023, 3, 532−539

nanoparticles, the increase of the potential is almost 25%. The latter produces a second factor for preventing particle agglomeration. As the electrostatic force scales linearly with V, $CoFe_2O_4$ coated with OA particles can withstand almost 4 times larger attractive forces, indicating a larger range of stability.

4. CONCLUSIONS

We have performed DFT calculations for magnetocrystalline anisotropy, magnetic moments, charge, and the electrostatic potential of Co ferrite and γ-Fe_2O_3 nanoparticles covered with OA and DEG for surface coverage up to 20%. Our findings demonstrate that OA results in the decrease of the mean magnetic moment for both particles as the coating coverage increases. For $CoFe_2O_4$, a reduction of the moment per atom is found mainly on B sites as Fe_B shows a reduced moment from 4.1 μ_B to 3.8 μ_B for 20% OA and Co_B from 2.7 to 2.6 μ_B. On the other hand, Fe_A shows a smaller variance from 4.2 to 4.15 μ_B. For Fe_2O_3, the B sites are the ones mainly affected by the coating as Fe_B shows a reduced moment from 4.0 to 3.91 μ_B. For the total net moment, a decrease of ∼4.5% is found for $CoFe_2O_4$ and ∼9.5% for Fe_2O_3 at 20% OA coverage.

The magnetocrystalline anisotropy shows different behavior. It significantly decreases for $CoFe_2O_4$ as the OA coverage percentage increases. Interestingly, for Fe_2O_3 a significant increase of the magnetic anisotropy is found, reaching an enhancement factor of ∼4.5 for 20% OA coverage. This is attributed to different types of ions being attached to the coating molecules. DEG variations of both the magnetic moment and the magnetic anisotropy are not significant since the DEG shows a weaker attachment on the surface than OA molecules by almost 1 eV. The latter is attributed to the different functional groups of the coatings, COOH for OA and OH for DEG.

We note that for the exchange interactions in both systems, the interaction between A′−B′ sites is increased, indicating an enhanced AF order compared with that of the uncoated nanoparticles. On the other hand, the A′−A′ and B′−B′ interactions decrease. This behavior is opposite to the one reported for the coated particles of ref 21 and indicates that the J_{ij}'s are sensitive not only to the type of atoms attached but also the shape of the particle as it can modify the coordination of the TM atoms.

As COOH shows a larger percentage of covalent bonding than OH, larger amount of charge is transferred to both particles when OA is attached on their surface rather than DEG. For 20% OA coverage, $CoFe_2O_4$ particles show a charge of 0.018e, whereas Fe_2O_3 particles show a charge of 0.01e. Notably for $CoFe_2O_4$, a larger variance of charge is found on the TM ions, while it is almost negligible for O atoms. Although, for Fe_2O_3 also the O atoms are strongly affected, and thus a smaller total charge is found.

The larger charge found on the $CoFe_2O_4$ particles leads to a larger tail of the electrostatic potential outside the particle, increasing the colloidal stability of $CoFe_2O_4$ with the same coverage.

ASSOCIATED CONTENT

Supporting Information

The Supporting Information is available free of charge at https://pubs.acs.org/doi/10.1021/acsphyschemau.3c00026.

Energies for the bidentate mode of OA attached to both particle types and structures of the highest coverage percentage for both ligands OA and DEG and for both particle types (PDF)

AUTHOR INFORMATION

Corresponding Author

Kalliopi N. Trohidou − *Institute of Nanoscience and Nanotechnology, NCSR "Demokritos", Attiki 153 10, Greece;* orcid.org/0000-0002-6921-5419; Email: k.trohidou@inn.demokritos.gr

Author

Nikolaos Ntallis − *Institute of Nanoscience and Nanotechnology, NCSR "Demokritos", Attiki 153 10, Greece;* orcid.org/0000-0002-4444-6819

Complete contact information is available at: https://pubs.acs.org/10.1021/acsphyschemau.3c00026

Notes

The authors declare no competing financial interest.

ACKNOWLEDGMENTS

The authors acknowledge the support from the Horizon Europe EIC Pathfinder Open Programme: under grant agreement no. 101046909 (REMAP) and computational time granted from the Greek Research & Technology Network (GRNET) in the National HPC facility ARIS (https://hpc.grnet.gr) under project REPROOF (pr. 13025). The authors gratefully thank Dr. C. Sangregorio (INSTM and CNR-ICCOM, 50019 Sesto Fiorentino (Firenze), Italy) and Prof. D. Peddis (Institute of Structure of Matter, National Research Council (CNR), Monterotondo Scalo, 00015 Rome, Italy, Department of Chemistry and Industrial Chemistry, University of Genova, 16146 Genova, Italy) for useful discussions on the types of nanoparticles and coatings.

REFERENCES

(1) Veiseh, O.; Gunn, J. W.; Zhang, M. Design and fabrication of magnetic nanoparticles for targeted drug delivery and imaging. *Adv. Drug Delivery Rev.* **2010**, *62*, 284.

(2) Cao, B.; Tang, Q.; Cheng, G. Recent advances of zwitterionic carboxybetaine materials and their derivatives. *J. Biomater. Sci., Polym. Ed.* **2014**, *25*, 1502−1513.

(3) Mushtaq, M. W.; Kanwal, F.; Imran, M.; Ameen, N.; Batool, M.; Batool, A.; Bashir, S.; Abbas, S. M.; Ur Rehman, A.; Riaz, S.; Naseem, S.; Ullah, Z. Synthesis of surfactant-coated cobalt ferrite nanoparticles for adsorptive removal of acid blue 45 dye. *Mater. Res. Express* **2018**, *5*, 035058.

(4) Vasilakaki, M.; Chikina, I.; Shikin, V. B.; Ntallis, N.; Peddis, D.; Varlamov, A. A.; Trohidou, K. N. Towards high-performance electrochemical thermal energy harvester based on ferrofluids. *Appl. Mater. Today* **2020**, *19*, 100587.

(5) Scherer, C.; Figueiredo Neto, A. M. Ferrofluids: properties and applications. *Braz. J. Phys.* **2005**, *35*, 718−727.

(6) Wang, R.; Han, F.; Chen, B.; Liu, L.; Wang, S.; Zhang, H.; Han, Y.; Chen, H. Liquid Nanoparticles: Manipulating the Nucleation and Growth of Nanoscale Droplets. *Angew. Chem., Int. Ed.* **2021**, *60*, 3047−3054.

(7) Gutiérrez, L.; De La Cueva, L.; Moros, M.; Mazarío, E.; De Bernardo, S.; De La Fuente, J. M.; Morales, M. P.; Salas, G. Aggregation effects on the magnetic properties of iron oxide colloids. *Nanotechnology* **2019**, *30*, 112001.

(8) Vasilakaki, M.; Ntallis, N.; Yaacoub, N.; Muscas, G.; Peddis, D.; Trohidou, K. N. Optimising the magnetic performance of Co ferrite nanoparticles via organic ligand capping. *Nanoscale* **2018**, *10*, 21244−21253.
(9) Berkowitz, A. E.; Lahut, J. A.; Jacobs, I. S.; Levinson, L. M.; Forester, D. W. Spin pinning at ferrite-organic interfaces. *Phys. Rev. Lett.* **1975**, *34*, 594−597.
(10) Bohara, R. A.; Thorat, N. D.; Yadav, H. M.; Pawar, S. H. One-step synthesis of uniform and biocompatible amine functionalized cobalt ferrite nanoparticles: a potential carrier for biomedical applications. *New J. Chem.* **2014**, *38*, 2979.
(11) Mourdikoudis, S.; Kostopoulou, A.; LaGrow, A. P. Magnetic nanoparticle composites: Synergetic effects and applications. *Adv. Sci.* **2021**, *8*, 2004951.
(12) Dippong, T.; Levei, E. A.; Cadar, O. Recent advances in synthesis and applications of MFe_2O_4 (M = Co, Cu, Mn, Ni, Zn) nanoparticles. *Nanomaterials* **2021**, *11*, 1560.
(13) Verma, H.; Mekuria, T.; Seck, P.; Hong, H.; Karna, S. P.; Seifu, D. Proximity effect tuned magnetic properties in composites of carbon nanotubes and nanoparticles of $CoFe_2O_4$. *J. Magn. Magn. Mater.* **2020**, *501*, 166438.
(14) Farkaš, B.; Terranova, U.; de Leeuw, N. H. Binding modes of carboxylic acids on cobalt nanoparticles. *Phys. Chem. Chem. Phys.* **2020**, *22*, 985−996.
(15) Vasilakaki, M.; Ntallis, N.; Trohidou, K. N. Tuning the magnetic properties of oleic-acid-coated cobalt ferrite nanoparticles by varying the surfactant coverage. *J. Phys. Chem. Solids* **2023**, *180*, 111424.
(16) Xu, H.; Wang, X.; Zhang, L. Selective preparation of nanorods and micro-octahedrons of Fe_2O_3 and their catalytic performances for thermal decomposition of ammonium perchlorate. *Powder Technol.* **2008**, *185*, 176−180.
(17) Yetter, R. A.; Risha, G. A.; Son, S. F. Metal particle combustion and nanotechnology. *Proc. Combust. Inst.* **2009**, *32*, 1819−1838.
(18) Yuan, Y.; Jiang, W.; Wang, Y.; Shen, P.; Li, F.; Li, P.; Zhao, F.; Gao, H. Hydrothermal preparation of Fe_2O_3/graphene nanocomposite and its enhanced catalytic activity on the thermal decomposition of ammonium perchlorate. *Appl. Surf. Sci.* **2014**, *303*, 354−359.
(19) Wu, W.; He, Q.; Jiang, C. Magnetic iron oxide nanoparticles: Synthesis and surface functionalization strategies. *Nanoscale Res. Lett.* **2008**, *3*, 397.
(20) Salafranca, J.; Gazquez, J.; Pérez, N.; Labarta, A.; Pantelides, S. T.; Pennycook, S. J.; Batlle, X.; Varela, M. Surfactant Organic Molecules Restore Magnetism in Metal-Oxide Nanoparticle Surfaces. *Nano Lett.* **2012**, *12*, 2499−2503.
(21) Bianchetti, E.; Di Valentin, C. Effect of Surface Functionalization on the Magnetization of Fe3O4 Nanoparticles by Hybrid Density Functional Theory Calculations. *J. Phys. Chem. Lett.* **2022**, *13*, 9348−9354.
(22) Limaye, M. V.; Singh, S. B.; Date, S. K.; Kothari, D.; Reddy, V. R.; Gupta, A.; Sathe, V.; Choudhary, R. J.; Kulkarni, S. K. High coercivity of oleic acid capped $CoFe_2O_4$ nanoparticles at room temperature. *J. Phys. Chem. B* **2009**, *113*, 9070−9076.
(23) Jovanović, S.; Spreitzer, M.; Tramsek, M.; Trontelj, Z.; Suvorov, D. Effect of oleic acid concentration on the physicochemical properties of Cobalt ferrite nanoparticles. *J. Phys. Chem. C* **2014**, *118*, 13844−13856.
(24) Kresse, G.; Furthmüller, J. Efficient iterative schemes for ab initio total-energy calculations using a plane-wave basis set. *Phys. Rev. B: Condens. Matter Mater. Phys.* **1996**, *54*, 11169−11186.
(25) Kresse, G.; Furthmüller, J. Efficiency of ab-initio total energy calculations for metals and semiconductors using a plane-wave basis set. *Comput. Mater. Sci.* **1996**, *6*, 15−50.
(26) Naumann, R. J. *Introduction to the Physics and Chemistry of Materials*; CRC Press Taylor and Francis Group: Boca Roton, 2008.
(27) Dudarev, S. L.; Botton, G. A.; Savrasov, S. Y.; Humphreys, C. J.; Sutton, A. P. Electron-energy-loss spectra and the structural stability of nickel oxide: An LSDA+U study. *Phys. Rev. B: Condens. Matter Mater. Phys.* **1998**, *57*, 1505−1509.
(28) Tang, W.; Sanville, E.; Henkelman, G. A grid-based Bader analysis algorithm without lattice bias. *J. Phys.: Condens. Matter* **2009**, *21*, 084204.
(29) Salazar-Alvarez, G.; Qin, J.; Šepelák, V.; Bergmann, I.; Vasilakaki, M.; Trohidou, K. N.; Ardisson, J. D.; Macedo, W. A. A.; Mikhaylova, M.; Muhammed, M.; Baró, M. D.; Nogués, J. Cubic versus Spherical Magnetic Nanoparticles: The Role of Surface Anisotropy. *J. Am. Chem. Soc.* **2008**, *130*, 13234−13239.
(30) López-Ortega, A.; Lottini, E.; Fernández, C. d. J.; Sangregorio, C. Exploring the magnetic properties of Cobalt-ferrite nanoparticles for the development of a rare-earth-free permanent magnet. *Chem. Mater.* **2015**, *27*, 4048−4056.
(31) Russel, W. B.; Saville, D. A.; Schowalter, W. R. *Colloidal Dispersions*; Cambridge University Press: Cambridge, 1991.

https://doi.org/10.1021/acsphyschemau.3c00026
ACS Phys. Chem Au 2023, 3, 532−539